IL NUOVO CIMENTO **41 C** (2018) 103
DOI 10.1393/ncc/i2018-18103-y

COMMUNICATIONS: SIF Congress 2017

Time-evolution and dynamics of Floquet edge states in irradiated graphene nanoribbons

M. PUVIANI(*)
Università degli Studi di Modena e Reggio Emilia - Modena, Italy

received 25 January 2018

Summary. — We study the solution of the time-dependent Schrödinger equation for systems driven out of equilibrium by a time-periodic laser field, using the Floquet equation as a mathematical tool to efficiently obtain the desired time-dependent observables. We calculate the velocity and charge of occupied states in a laser-irradiated zig-zag graphene nanoribbon (zGNR), focusing on the role and properties of topologically protected edge states: their robustness against defects and disorder is tested, as well as their behavior when a bias voltage is applied across a section of the ribbon. Our results reveal the importance of the time-dependent approach to correctly calculate observables of laser-driven materials according to the occupation of states, suggesting how the properties of protected edge-states can be exploited to create flying-qubit architectures.

1. – Introduction

The continuous application of an intense homogeneous laser field drives the electrons of an atomic lattice out of equilibrium into a time-periodic quasi-steady state, which is called Floquet state. Indeed, this can be theoretically treated with the Floquet theory, based on the equivalent of the Bloch theorem in time domain, to describe properly the photon-dressed electrons of the system [1-3]. Furthermore, under some circumstances of intensity and polarization, it is possible to induce a phase transition from a trivial to a non-trivial topological behaviour [4-9]. In particular, the generation and manipulation of topological states through the application of a time-periodic perturbation has been experimentally demonstrated in different systems such as ultra-cold gases in time-dependent optical lattices [10], periodically driven photonic waveguide lattices [11, 12] and topological insulators under circularly polarized light [13].

In our work we consider the prototypical case of irradiated graphene: this system is a trivial semimetal in equilibrium condition, but it becomes a 2D Chern insulator (namely it

(*) E-mail: matteo.puviani@unimore.it

shows a gap in 2D and linear dispersive edge states in 1D) when irradiated by circularly polarized light [14]. Zig-zag graphene nanoribbons are characterized by Floquet edge states which are topologically protected and responsible of a quantized Hall conductance in the absence of a magnetic field, a remarkable realization of the so-called "quantum Hall systems without Landau levels" originally proposed by Haldane.

In the present paper, we focus on the time evolution of observables calculated in the Floquet states of laser-driven graphene nanoribbons by calculating the time-evolution of the charge in real-space associated to the time-periodic dynamics of those states. In addition, we explore the real-space dynamics of a particle initialized into these edge states, showing how time evolution is affected by local defects, disorder and potential barriers applied across the nanoribbon.

2. – Theoretical development

2˙1. *Floquet-Bloch theory for periodically driven lattices.* – A system described by a quantum state $|\Psi(t)\rangle$ which evolves according to an explicitely time-dependent Hamiltonian $\hat{H}(t)$ is the solution of the Schrödinger equation, namely

$$\hat{H}(t)|\Psi(t)\rangle = i\frac{\partial}{\partial t}|\Psi(t)\rangle. \tag{1}$$

The single-particle tight-binding Hamiltonian used to describe an atomic lattice interacting with an external periodic driving reads

$$\hat{H}_{\mathbf{k}}(t) = \sum_{i,j} J_{i,j}\ e^{i(\mathbf{k}+\mathbf{A}(t))\cdot(\mathbf{r}_i-\mathbf{r}_j)}\ \hat{c}_i^{\dagger}(t)\ \hat{c}_j(t), \tag{2}$$

where $\mathbf{A}(t)$ is the vector potential of the laser field. Here we have used the minimal coupling [15], which transforms the nearest-neighbors hopping integral $J_{i,j}$ into $J_{i,j}\ e^{i\mathbf{A}(t)\cdot(\mathbf{r}_i-\mathbf{r}_j)}$. Moreover, the creation and annihilation operators themeselves contain the intrinsic time-periodic part of the evolution.

Due to the spatial and temporal periodicity of the irradiated lattice we can make use of both the Bloch and Floquet theorems to write the solution of eq. (1) as follows:

$$\Psi_{\alpha,\mathbf{k}}(\mathbf{r},t) = e^{-i\varepsilon_\alpha(\mathbf{k})t}\ e^{i\mathbf{k}\cdot\mathbf{r}}\ \Phi_{\alpha,\mathbf{k}}\ (\mathbf{r},t), \tag{3}$$

with $\Phi_{\alpha,\mathbf{k}}\ (\mathbf{r},t) = \Phi_{\alpha,\mathbf{k}}\ (\mathbf{r},t+T) = \Phi_{\alpha,\mathbf{k}}\ (\mathbf{r}+\mathbf{R},t)$, $\mathbf{R}$ being the lattice vector, $T = 2\pi/\Omega$ the period of the external driving with frequency Ω. Here we have written the wave function starting from the Dirac notation $\langle\mathbf{r}|\Psi_{\alpha,\mathbf{k}}(t)\rangle = \Psi_{\alpha,\mathbf{k}}(\mathbf{r},t)$. Furthermore, the time- and space-periodic solution of the Schrödinger equation can be expanded in Fourier series in time and in a spatially localized basis set as follows:

$$\Phi_{\alpha,\mathbf{k}}\ (\mathbf{r},t) = \sum_{n=-\infty}^{+\infty}\sum_{i=1}^{N} c_{i,n}^{\alpha}(\mathbf{k})\ e^{-in\Omega t}\ e^{-i\mathbf{k}\cdot\mathbf{r}_i}\ \varphi(\mathbf{r}-\mathbf{r}_i). \tag{4}$$

Defining the Floquet Hamiltonian as the operator $\hat{H}_F \equiv \hat{H}(t) - i\frac{\partial}{\partial t}$, the Schrödinger equation in (1) can be rewritten in order to obtain the so-called Floquet equation, which

is an eigenvalue problem for the periodic part of the Schr'odinger solution:

$$\hat{H}_F \ \Phi_{\alpha,\mathbf{k}}(\mathbf{r},t) = \varepsilon_\alpha(\mathbf{k}) \ \Phi_{\alpha,\mathbf{k}}(\mathbf{r},t). \tag{5}$$

The eigenvalue, which is the Floquet quasi-energy, appears in the exponent of the time envelope function in (3). It is important to realize that the Floquet eigenvalue is constant in time and therefore is a conserved quantity, contrary to the energy.

The Floquet operator for the tight-binding Hamiltonian in (2) reads

$$\hat{H}^F_{\mathbf{k}} = \sum_{i,j} \sum_{n,m=-\infty}^{+\infty} J_{ij,nm} \ e^{i\mathbf{k}\cdot(\mathbf{r}_i-\mathbf{r}_j)} \ \hat{c}^\dagger_{i,n} \ \hat{c}_{j,m} - n \ \Omega \ \delta_{n,m}\delta_{i,j}, \tag{6}$$

where $J_{ij,nm} = \frac{1}{T}\int_0^T J_{ij} \ e^{i\frac{\mathbf{A}(t)}{A_0}\cdot(\mathbf{r}_i-\mathbf{r}_j)-in\Omega t} \ \mathrm{d}t$ is the modified hopping.

2˙2. *Evolution of states and time-dependent observables.* – The time-dependent energy of the electrons, which is not conserved in time, can be calculated as the expectation value of the Hamiltonian operator for the full solution of the Schrödinger equation, namely $\langle\Psi_{\alpha\mathbf{k}}(t)|\hat{H}(t)|\Psi_{\alpha\mathbf{k}}(t)\rangle$. The result can be written in terms of the Floquet quasi-energy and the Floquet states:

$$\mathrm{E}_\alpha(\mathbf{k},t) = \varepsilon_\alpha(\mathbf{k}) + \sum_{n,m=-\infty}^{+\infty} e^{i(n-m)\Omega t} \ m \ \Omega \left| \sum_i c^\alpha_{i,n}(\mathbf{k}) \right|^2. \tag{7}$$

Similarly, other time-dependent observables can be calculated, *e.g.* the charge density, defined as

$$\rho(\mathbf{r}_i,t,t_0) = \langle\Psi(t_0)|\hat{c}^\dagger_i(t)_H\hat{c}_i(t)_H|\Psi(t_0)\rangle. \tag{8}$$

From eq. (8) it appears clearly that the charge density, as well as any ground state expectation value, depends both on t and t_0, the instant at which the system is initialized. Thus, using the Floquet solution (4) in expression (8) we get

$$\rho(\mathbf{r}_i,t,t_0) = \sum_{\mathbf{k}} \sum_{\alpha\in\mathcal{G}_\mathbf{k}(t_0)} \sum_{n,m} e^{i(n-m)\Omega t} \ c^{\alpha*}_{i,n}(\mathbf{k}) \ c^\alpha_{i,m}(\mathbf{k}). \tag{9}$$

Here we have to pay attention to the summation of the energy levels α, which is performed over the set of levels whose energy is non-positive at time t_0, which is $\mathcal{G}_\mathbf{k}(t_0) = \{\alpha : E_\alpha(\mathbf{k},t_0) \leq 0\}$. This physically means that we took the equilibrium distribution as the initial population of the system. Actually, experimentally it is not possible to fix the initial time with respect to the external periodic driving: an average over the possible initial state is more appropriate, that is

$$\rho(\mathbf{r}_i,t) = \frac{1}{T}\int_0^T \rho(\mathbf{r}_i,t,t_0) \ \mathrm{d}t_0. \tag{10}$$

Another way to proceed is to assume that at each time the ground state is the one of minimum energy, so that the time-dependent charge density becomes

$$\tilde{\rho}(\mathbf{r}_i, t) = \sum_{\mathbf{k}} \sum_{\alpha \in \mathcal{G}_{\mathbf{k}}(t)} \sum_{n,m} e^{i(n-m)\Omega t}\ c^{\alpha *}_{i,n}(\mathbf{k})\ c^{\alpha}_{i,m}(\mathbf{k}), \tag{11}$$

where the summation of the energy levels α is performed over those which belongs to the set $\mathcal{G}_{\mathbf{k}}(t) = \{\alpha : E_\alpha(\mathbf{k}, t) \leq 0\}$. This assumption corresponds to neglect the time-dependent electronic excitations associated to the external driving. The quantitative difference $\Delta\rho(t) = \rho(\mathbf{r}_i, t) - \tilde{\rho}(\mathbf{r}_i, t)$ between the two approaches can reveal the nature and the importance of these time-periodic excitations.

2˙3. *Electron dynamics of driven systems in real space and time.* – The time-evolution operator can be written in real space using the form suggested by the Floquet theorem for the solution of the Schrödinger equation [1] as

$$U_{i,j}(t, t_0) = \sum_{\alpha} \sum_{n,m=-\infty}^{+\infty} e^{-i\varepsilon_\alpha (t-t_0)}\ e^{-im\Omega t}\ e^{in\Omega t_0}\ c^{\alpha}_{j,m}\ c^{\alpha *}_{i,n}. \tag{12}$$

Then the probability for an electron of being on site i at time t if it was on site j at time t_0 is simply given by $|U_{i,j}(t, t_0)|^2$.

The dynamics in real space and time, described as the probability of going from one site to another of the lattice, averaging over the initial time t_0 and keeping fixed the time interval $t - t_0$ is given by

$$P_{j \leftarrow i}(t) = \mathcal{N} \sum_{n=-\infty}^{+\infty} \left| \sum_{\mathbf{k}} \sum_{\alpha \in \mathcal{E}_{\mathbf{k}}} c^{\alpha}_{i,0}(\mathbf{k})^*\ c^{\alpha}_{j,n}(\mathbf{k})\ e^{i\mathbf{k}\cdot(\mathbf{r}_i - \mathbf{r}_j)}\ e^{-i\varepsilon_\alpha(\mathbf{k})t} \right|^2. \tag{13}$$

Since we want to study a one-dimensional system infinite along one direction, the k-vector is $\mathbf{k} = k\,\hat{i}$ along the x axis, and in particular $k = k_n = \frac{n\pi}{Na}$, with $n \in \{0, \pm 1, \pm 2, \ldots, \pm N\}$, a being the lattice parameter of the extended cell of the nanoribbon. So we can choose the cell large enough and the edge states with k close enough to each other and to the center of the BZ so that $k_n \approx k \approx 0$, and thus we can write expression (13) as follows [16]:

$$P_{j \leftarrow i}(t) = \mathcal{N} \sum_{n=-\infty}^{+\infty} \left| \sum_{k \approx 0} \sum_{\alpha \in \mathcal{E}_k} c^{\alpha}_{i,0}(k)^*\ c^{\alpha}_{j,n}(k)\ e^{-i\varepsilon_\alpha(k)t} \right|^2. \tag{14}$$

3. – Numerical results

3˙1. *Floquet states of driven zGNR.* – We first studied the Floquet states of photon-dressed electron quasiparticles in graphene, starting from the time-dependent driven Hamiltonian as expressed in eq. (2), with the nearest-neighbour hopping parameter which is $J_{i,j} = 2.8\,\mathrm{eV}$. In particular, we focused on the effects of reduced dimensionality, namely on the gapless edge states that arise in driven graphene nanoribbons. In order to do that we chose a zig-zag terminated 50-atoms wide ribbon with high frequency ($\Omega = 12\,\mathrm{eV}$,

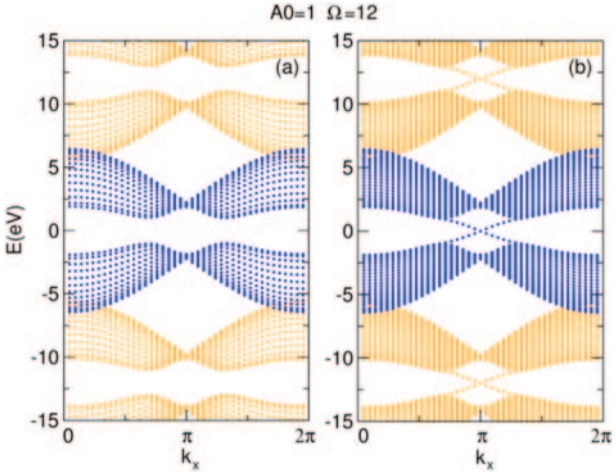

Fig. 1. – Floquet quasi-energies band structure for circularly polarized light with $\Omega = 12\,\mathrm{eV}$ and $A_0 = 1.0$ in units of the carbon-carbon distance. On the left the plot represents the Floquet Projected Bulk Band Structure (FPBBS) as described in the text, on the right the Floquet sidebands dispersion for the zig-zag graphene nanoribbon. The blue dots refer to the zero-mode of Floquet band, while in orange are shown the other Floquet sidebands, replicated at $\pm n\Omega$.

i.e. $\Omega/J \simeq 4$) and high intensity ($A_0 = 1.0$ in units of the inverse carbon-carbon distance([1]) [17]).

In fig. (1) there is a comparison of the Floquet quasi-energies obtained for the honeycomb lattice in 2D and 1D exposed to a circularly polarized field $\mathbf{A}(t) = A_0(\cos(\Omega t)\hat{i} + \sin(\Omega t)\hat{j})$. Panel (a) reports the Floquet Projected Bulk Band Structure (FPBBS), namely the Floquet eigenvalues obtained for the 2D lattice using the same unit cell of the ribbon and periodically repeated in both x and y directions (along the ribbon and perpendicularly to it), in this way restoring the 2D translation symmetry. As currently done in standard surface physics [18], the projected bulk band structure allows to identify straightaway the energy regions that, prohibited in the bulk, can host localized states at the edges. Panel (b), instead, shows the Floquet quasi-energies obtained in the 1D ribbon geometry clearly characterized by extra states in the 2D forbidden regions. These gapless edge states go in pairs being localized either on the upper or on the lower margin of the ribbon and exhibit the peculiar linear dispersion evocative of a non-trivial topological character [19-21].

3˙2. *Time evolution of irradiated zGNR.* – Studying the same system of 50-atoms wide zig-zag graphene nanoribbon irradiated by a spatially homogeneous laser field, we performed some systematics for different conditions of frequency regime and polarization. For all of them we analyzed the time evolution of the expectation values of the energy of edge-localized states and the charge dynamics across the nanoribbon. Specifically, we were interested in calculating the time-dependent energy as in (7), focusing only on those states which are localized at the edges of the nanoribbon itself. As it appears

([1]) $A_0 = 1.0$ in units of the C-C distance corresponds for graphene to $A_0 = 4.6 \cdot 10^{-6}\,\mathrm{J\,s\,C^{-1}\,m^{-1}}$.

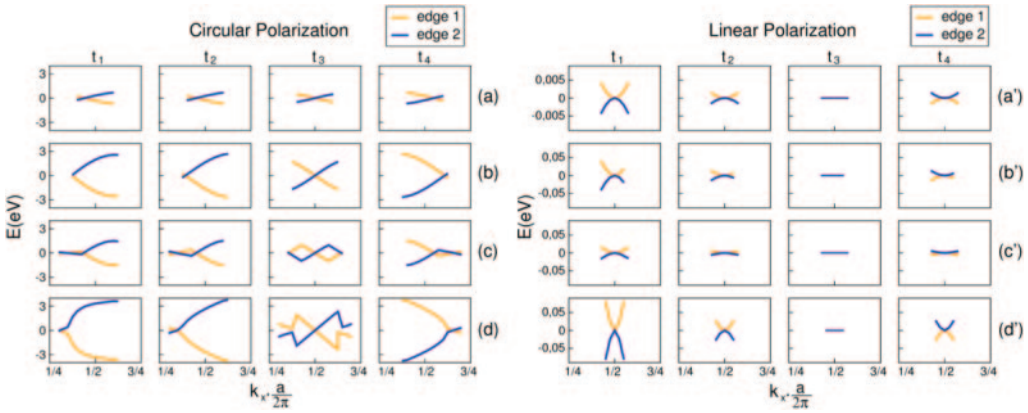

Fig. 2. – Evolution in time of the band dispersion of the states localized on the nanoribbon edges, under the driving of circularly (panels on the left) and linearly (on the right side) polarized light. Results are provided for different regimes of frequency and intensity at times $t_n = (2\pi/\Omega) \cdot [(n-1)/8]$. In particular, for panels (a) and (a) $\Omega = 12\,\mathrm{eV}$ and $A_= = 0.5$, (b) and (b) $\Omega = 12\,\mathrm{eV}$ and $A_= = 1.0$; (c) and (c) $\Omega = 5.5\,\mathrm{eV}$ and $A_= = 0.5$; (d) and (d) $\Omega = 5.5\,\mathrm{eV}$ and $A_= = 1.0$.

in fig. 2, with circular polarization in the high-frequency regime (panels (a) and (b)), which corresponds to $\Omega/J \gg 1$ such as in the case of $\Omega = 12\,\mathrm{eV}$, the two edge states keep the same k-dispersion in time with the same slope but different energy values. This corresponds to the two unidirectional states moving along each edge of the nanoribbon with a velocity which is constant in time. For smaller frequencies, instead, such as that corresponding to a photon energy $\Omega = 5.5\,\mathrm{eV}$ shown in panels (c) and (d), the edge states show a more complicated k-dispersion, with non-constant slope and kinks. In these cases, however, for low frequency and high intensity of the driving field ($A_0 = 1$, panel (d)), the states are less localized than in the previous ones.

The effect of linearly polarized radiation, instead, is significantly different on the edge states: indeed, they are confined in a shorter region of the BZ and they show a non-linear dispersion which is reduced of orders of magnitude with respect to the case of circular polarization. This physically means that the left-mover/right-mover behaviour is lost, with a dispersion which is actually parabolic (even though almost flat).

3˙3. *Charge and excitations dynamics in time.* – In the light of these results, we computed the time-dependent expectation value of the charge density on each atom across the nanoribbon, for the same regimes of frequency and intensity of the external driving as above. We used both equations (10) and (11), since interesting physical considerations can be obtained from them.

As can be realized from fig. 3, for circular polarization and high frequency the difference between the two calculations of the charge density is higher: it physically means that electronic excitations are more important in this regime, and for lower intensities they are mainly localized on the edge atoms. Additionally, the overall charge imbalance between neighbouring sites is decreased due to the excitations of states, as can be seen comparing the two calculations. On the other hand, for linearly polarized light there is no substantial difference, apart from a lower charge excitation on the boundary atoms.

Lowering the frequency to $\Omega = 5.5\,\mathrm{eV}$ the charge excitations are mainly delocalized across all the nanoribbon, both for circular and linear polarization of the driving field,

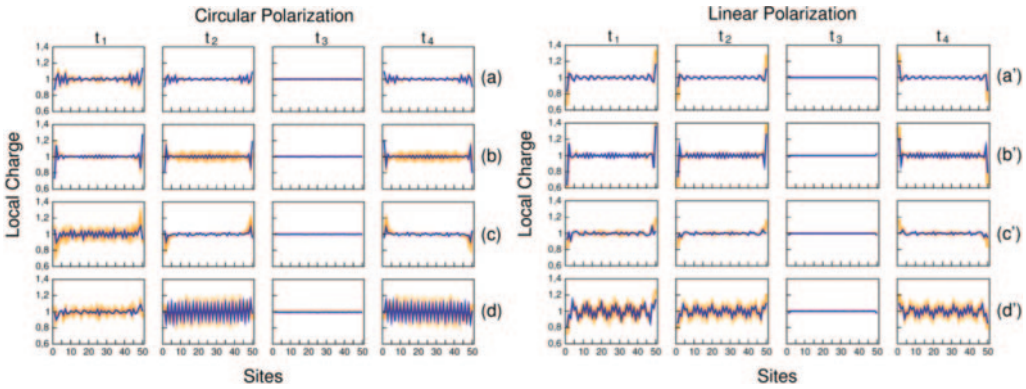

Fig. 3. – Dynamics in time of the local charge across the 50-atoms wide zGNR, for circularly (panels on the left side) and linearly (on the right) polarized radiation in different regimes of frequency and intensity. In particular, for panels (a) and (a) $\Omega = 12\,\mathrm{eV}$ and $A_0 = 0.5$ (in units of C-C distance), (b) and (b) $\Omega = 12\,\mathrm{eV}$ and $A_0 = 1.0$; (c) and (c) $\Omega = 5.5$ eV and $A_0 = 0.5$; (d) and (d) $\Omega = 5.5\,\mathrm{eV}$ and $A_0 = 1.0$. The charge values are provided at times $t_n = (2\pi/\Omega) \cdot [(n-1)/8]$, with $n = 1, 2, 3, 4$. In orange the $\rho(\mathbf{r}_i, t)$ is shown, in blue $\rho(\tilde{\mathbf{r}_i}, t)$.

in particular for higher intensities.

All in all, this allows us to conclude that it is possible to obtain electronic time-periodic oscillations up to $\sim 1/5$ of the charge on each atom applying a laser driving on a graphene nanoribbon, and that electronic excitations arise predominantly with circular polarization and high frequency. In this regime the excitations are mostly localized on the edges of the nanoribbon, while they become delocalized for lower frequencies. Moreover, this clarifies the role of the edge states: since they are located around the mid-band k-dispersion, their weight is higher for high frequencies, when the Floquet sidebands are far apart from each other and multi-photon processes are almost negligible. When the frequency is lowered, on the contrary, even the low-energy band levels become relevant as multi-photon processes are more probable and so is their excitation.

3˙4. *Dynamics with localized defects and noise.* – So far we have characterized the evolution of energy and charge of time-dependent states localized at the edges of irradiated graphene nanoribbons. In the light of these results, we decided to simulate the dynamics of an electron wavepacket initialized into edge states on the margin of the nanoribbon, in a 48×51 atoms-wide zig-zag terminated supercell with periodic boundary conditions along the x axis. We decided to focus on the prototypical case of circular polarization, high-frequency regime, *i.e.* $\Omega \gg J$ ($\Omega/J = 12$) and intense laser field ($A_0 = 1.0$). After checking that the wavepacket was correctly initialized and that its propagation was confined into the edge of the ribbon, we simulated its dynamics in a zGNR with edge vacancies, obtained removing tens of atoms on the boundary of the supercell. As can be seen from fig. 4, the wavepacket is perfectly transmitted around the defect without scattering or dissipation, confirming the topological character of the system.

However, thanks to versatility and efficiency of the theoretical framework that we used, we were able to add static noise to the irradiated nanoribbon. As is shown in fig. 5, adding a random on-site energy $E/J \in [0, 0.5]$ (panel on the top) there still are edge states: in the bottom panel the lower edge states are shown.

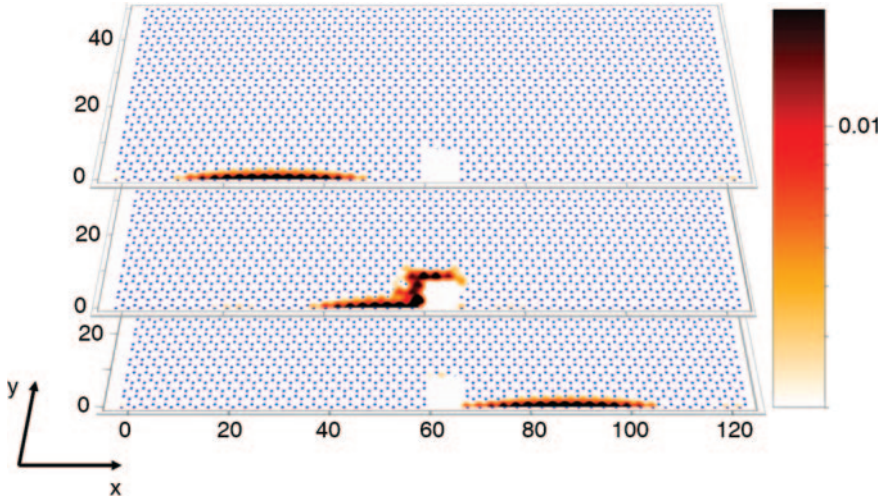

Fig. 4. – From top to bottom: snapshots at three different times of the evolution of an injected electron into a lower-edge pure state in the presence of vacancies (missing sites). The color map represents the probability to find the elctron on each site.

3˙5. *Control of edge states in laser-driven zGNR with potential barriers*. – In order to make a further step forward, we considered the same graphene nanoribbon under the same polarization and intensity conditions as in the previous section, adding a potential barrier across it, in order to control the dyanmics of the edge states. In particular, injecting an electron into a pure edge state (for example, into the lower edge), its dynam-

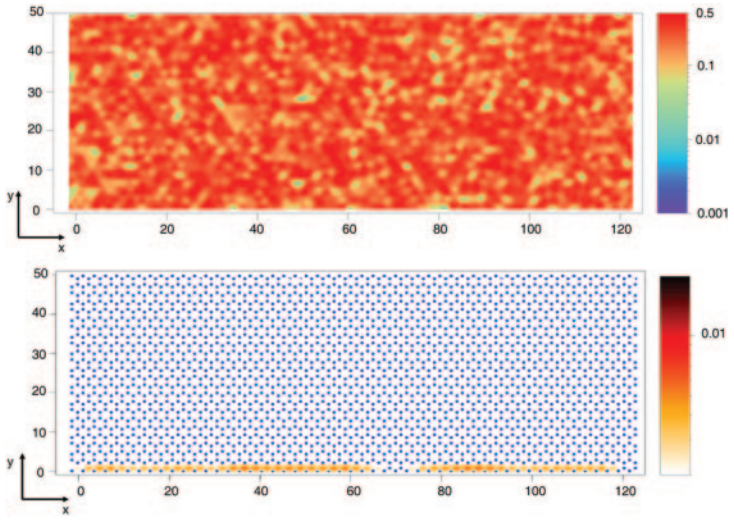

Fig. 5. – Top: color map of the random noise (as on-site random potential in $[0, 0.5]$) on the nanoribbon. Bottom: edge states localized on the lower margin of the nanoribbon: as can be seen, there is no scattering since their trace is localized only on the edge sites.

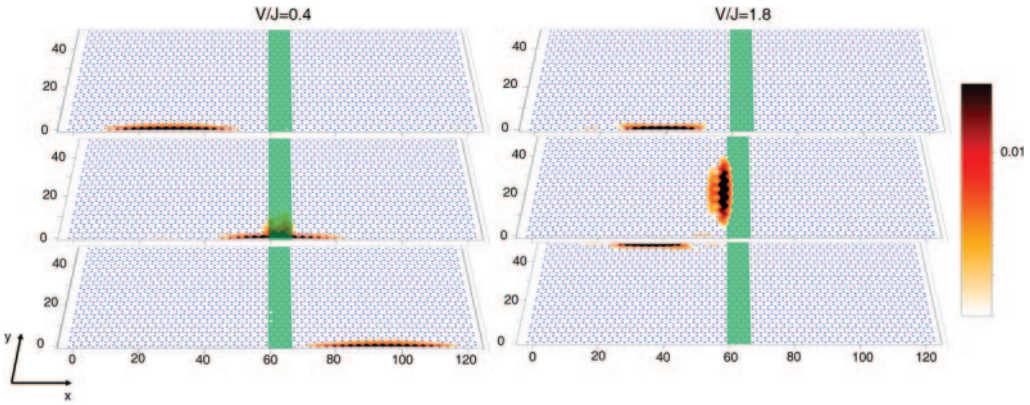

Fig. 6. – From top to bottom: snapshots at increasing time of the dynamics of an injected right-mover electron on the lower-edge state in the presence of a potential barrier (green): $V/J = 0.4$ on the left panels and $V/J = 1.8$ on the right.

ics can be influenced with a non-linear and non-trivial behavior by tuning the potential intensity [16]. In fig. 6 two cases are shown: on the left, when $V/J = 0.4$, the state is perfectly transmitted along the ribbon, since it cannot be backscattered onto the same edge due to the right-moving behaviour. However, for certain values of the potential barrier, the electron can be either perfectly reflected ($V/J = 1.8$, right panel of fig. 6) or splitted. The latter case occurs when there is a fair competition between the tunneling through the barrier and the tunneling between two edge states, crossing the nanoribbon along the barrier, with a mechanism which is evocative of the Klein tunneling. In this case however, the backscattering is soppressed by the topological character of the system, and occurs only when the opposite-moving edge on the other side of the ribbon is energetically favourable with respect to the tunneling of the barrier.

4. – Conclusion

In conclusion, we have shown in details the theoretical framework to study and characterize Floquet states in driven systems, their time evolution and their dynamics in space with an efficient scheme. Focusing on graphene nanoribbons, we have revealed that charge oscillations and time-dependent charge excitations occur when irradiated, performing a systematic calculation and characterization in different regimes of intensity and polarization of the driving electromagnetic field.

We have also simulated the dynamics of Floquet states in real space, demonstrating the topological robustness of edge states: indeed, they show perfect transmission and no scattering when defects or noise is applied to the system. Moreover, we have calculated the propagation of edge states when a potential barrier of different height is applied across the ribbon, in order to control their direction and dynamics.

* * *

This work was produced in collaboration with Prof. F. Manghi, from the University of Modena and Reggio Emilia, and Dr. A. Bertoni, from the CNR-Nano in Modena.

REFERENCES

[1] Shirley Jon H., *Phys. Rev. B*, **138** (1965) 979.
[2] Puviani M. and Manghi F., *Phys. Rev. B*, **94** (2016) 161111.
[3] Puviani M. and Manghi F., *J. Phys.: Conf. Ser.*, **841** (2017) 012021.
[4] Kitagawa Takuya, Oka Takashi, Brataas Arne, Fu Liang and Demler Eugene, *Phys. Rev. B*, **84** (2011) 235108.
[5] Oka Takashi and Aoki Hideo, *Phys. Rev. B*, **79** (2009) 081406.
[6] Lindner Netanel H., Refael Gil and Galitski Victor, *Nat. Phys.*, **7** (2011) 490.
[7] Inoue Jun-Ichi and Tanaka Akihiro, *Phys. Rev. Lett.*, **105** (2010) 017401.
[8] Rudner Mark S., Lindner Netanel H., Berg Erez and Levin Michael, *Phys. Rev. X*, **3** (2013) 031005.
[9] Harper Fenner and Roy Rahul, *Phys. Rev. Lett.*, **118** (2017) 115301.
[10] Goldman N., Budich J. C. and Zoller P., *Nat. Phys.*, **12** (2016) 639. Progress Article.
[11] Maczewsky Lukas J., Zeuner Julia M., Nolte Stefan and Szameit Alexander, *Nat. Commun.*, **8** (2017) 13756.
[12] Rechtsman Mikael C., Zeuner Julia M., Plotnik Yonatan, Lumer Yaakov, Podolsky Daniel, Dreisow Felix, Nolte Stefan, Segev Mordechai and Szameit Alexander, *Nature*, **496** (2013) 196.
[13] McIver J. W., Hsieh D., Steinberg H., Jarillo-Herrero P. and Gedik N., *Nat. Nanotechnol.*, **7** (2012) 96.
[14] Perez-Piskunow P. M., Foa Torres L. E. F. and Usaj Gonzalo, *Phys. Rev. A*, **91** (2015) 043625.
[15] Jiménez-García K., LeBlanc L. J., Williams R. A., Beeler M. C., Perry A. R. and Spielman I. B., *Phys. Rev. Lett.*, **108** (2012) 225303.
[16] Puviani M., Manghi F. and Bertoni A., *Phys. Rev. B*, **95** (2017) 235430.
[17] Sentef M. A., Claassen M., Kemper A. F., Moritz B., Oka T., Freericks J. K. and Devereaux T. P., *Nat. Commun.*, **6** (2015) 7047.
[18] Manghi F., Calandra C. and Molinari E., *Surf. Sci.*, **184** (1987) 449.
[19] Kane C. L. and Mele E. J., Z_2. *Phys. Rev. Lett.*, **95** (2005) 146802.
[20] Grandi F., Manghi F., Corradini O. and Bertoni C. M., *Phys. Rev. B*, **91** (2015) 115112.
[21] Grandi F., Manghi F., Corradini O., Bertoni C. M. and Bonini A., *New J. Phys.*, **17** (2015) 023004.